Nano Carbons 2024; 2(1): 298.
Original Research Article

The study of multilayer graphene membrane performance in O_2 purification process: Molecular dynamics simulation

Mohammad Pour Panah[1], Bahman Parvandar Asadollahi[2], Roozbeh Sabetvand[3,*]

[1] *Department of Physics, Faculty of Basic Sciences, Tarbiat Modares University, Tehran 14115-111, Iran*

[2] *Mechanical Engineering Department, Faculty of Engineering, Shahid Chamran University of Ahvaz, Ahvaz 61357-83151, Iran*

[3] *Department of Energy Engineering and Physics, Faculty of Condensed Matter Physics, Amirkabir University of Technology, Tehran 159163-4311, Iran*

*** Corresponding author:** Roozbeh Sabetvand, r.sabetvand@gmail.com

ARTICLE INFO

Received: 9 November 2023
Accepted: 26 February 2024
Available online: 9 April 2024

doi: 10.59400/n-c.v2i1.298

ABSTRACT: We use the molecular dynamics (MD) method to describe the atomic behavior of graphene nanostructures for oxygen molecules (O_2) separation from carbon dioxide (CO_2) molecules. Technically, for the simulation of the graphene-based membrane and O_2-CO_2 gas mixture, we used Tersoff and DREIDING force fields, respectively. The result of the equilibrium process of these structures indicated the good stability of them. Physically, this behavior arises from the appropriate MD simulation settings. Furthermore, to describe the purification performance of graphene-based membranes, we report some physical parameters such as purification value, impurity rate, and permeability of the membrane after the atomic filtering process. Numerically, by defined membrane optimization, the purification value of them reaches 97.31%. Also, by using these atomic structures, the CO_2 impurity that passed from the graphene-based membrane reached a zero value.

KEYWORDS: graphene; atomic membrane; molecular dynamics; purification process; oxygen; carbon dioxide

1. Introduction

Atomic membranes are a new class of low-dimensional, free-standing, physically stable, and virtually impermeable materials[1–4]. The common 2D atomic membrane is graphene nanosheet, a two-dimensional lattice entirely made of carbon atoms, but other interesting structures such as the multilayer graphene offer new properties[5–8]. Structurally, a graphene nanosheet is a layer of carbon atoms that are bonded together with covalent interaction in a honeycomb lattice. This atomic structure shows promising properties, including a high specific surface area, good thermal conductivity, proper mechanical behavior, and excellent charge mobility[9,10]. Due to these interesting properties, this atomic layer has remained at the core of scientific research since its advent, with many of its successful accomplishments being transformed into various applications. Today, graphene-based nanostructures are used commonly in fuel cells[11,12], supercapacitor[13,14], capacitive deionization[15–17], desalination[18–20]. Furthermore, graphene-based membranes are the other class of this atomic structure application. These atomic membranes are capable of creating an appropriate barrier when dealing with liquid and gas particles. Graphene-based membranes effectively separate target atoms from liquid and gaseous environments. Physically, due to the repulsive interaction of the π-bond orbital electron distribution in the graphene nanosheet, this atomic structure is not permeable to liquid or gas environment[21].

These practical properties of graphene membranes can be studied with experimental and theoretical approaches. Molecular Dynamics (MD) method is one of the important methods in the atomic study of various nanostructures[22–25]. Previously, this computational method was used for graphene-based membrane study. Cohen-Tanugi and Grossman[26] showed that nanoporous graphene membranes can remove NaCl from H_2O molecules. In their work, simulation results show the single-layer membrane delivery capacity reaches 66 L/(cm^2·day·MPa). In other work, this research group used single-layer graphene as a reference structure to explore the possibility of multilayer graphene membranes[27]. The result of this computational work shows the appropriate properties of multilayer graphene structures as atomic membranes. Kim et al.[28] described the transport of H_2O molecules and atomic ions in the pores of the graphene nanosheet. The MD results indicated the use of hydroxylated graphene pores can improve the membrane efficiency for actual applications. Also, Wang et al.[29] used a graphene nanosheet on a polyacrylonitrile matrix to introduce an effective graphene oxide membrane. It was found that with graphene oxide thickness increasing, the H_2O molecules flux decreased appreciably. So, due to the appropriate performance of MD simulations in the study of graphene-based membrane behavior, in this work we use this approach to describe the performance of a multilayer (3-layer) graphene membrane in the O_2 purification process from O_2-CO_2 gas mixture for the first time. In our MD simulations, the distance between various sheets and porous radius changes to designing optimized atomic membranes for the O_2 molecules purification process to actual applications.

2. Computational method

In this MD study, the graphene membrane and initial mixture gas (O_2-CO_2) interact with each other for t = 2 ns. This atomic procedure determines the graphene membrane filtering performance in the O_2 purification process. In our computational approach, simulations were done by the LAMMPS package[30–33]. By using this computational package, a multi-layer graphene membrane and O_2-CO_2 gas mixture simulated as C, H, and O atom arrangements as depicted in **Figure 1**. This atomic structure is depicted by OVITO (Open Visualization Tool) software[34]. Computationally, in depicted atomic structures, fixed boundary conditions were used in the x direction, and periodic style was implemented in the y and z directions[35]. After atomic modeling, the NVT ensemble was used in our MD simulations to equilibrate the temperature of structures[36,37]. This computational ensemble equilibrates the modeled samples at T_0 = 300 K with a 0.001 damping value for temperature.

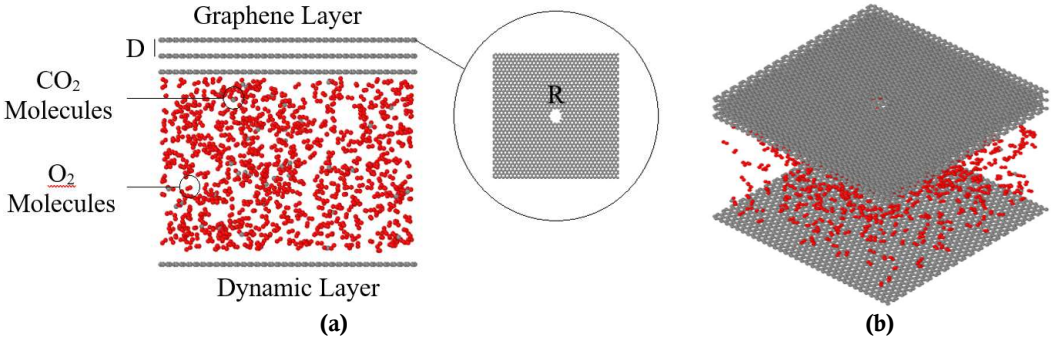

Figure 1. Multi-layer graphene membrane and O_2-CO_2 gas mixture simulated as C, H, and O atoms arrangement. **(a)** atomic properties of simulated structures with LAMMPS package; **(b)** atomic structures arrangement inside MD simulation box.

The atomic force field is an important parameter in common MD simulations. To simulate the atomic structures inside the MD box, we use DREIDING and Tersoff force-fields[38,39]. In the DREIDING force field, the atomic interactions were presented by non-bonded and bonded terms. The

non-bond term in atomic structure simulation is defined by the Lennard-Jones (LJ) equation (12-6 type) as reported in Equation (1). Historically, this mathematical function was introduced by John Lennard Jones for the first time as Equation (1)[40]:

$$E(r) = 4\varepsilon\left[\left(\frac{\sigma}{r_{ij}}\right)^{12} - \left(\frac{\sigma}{r_{ij}}\right)^{6}\right], \qquad r \ll r_c \tag{1}$$

In Equation (1), ε is the depth of the potential well, σ is the distance at which the potential function is zero, and r_{ij} is the atomic distance. These physical parameters are selected with the type of atoms in simulated structures. So, these parameters are valued for all atoms in our MD simulation reported in **Table 1**[39].

Table 1. The ε and σ constants for LJ interactions in our MD simulation box[39].

Type of atoms	σ (Å)	ε (kcal/mol)
C	4.180	0.3050
H	3.200	0.0100
O	3.710	0.4150

The bonded term of atomic interactions consists of simple and angle strengths. The bond and angle strengths in the DREIDING force field are calculated by harmonic oscillator formalism as Equations (2) and (3), respectively[39]:

$$E_r = \frac{1}{2}k_r(r - r_0) \tag{2}$$

$$E_\theta = \frac{1}{2}k_\theta(\theta - \theta_0) \tag{3}$$

In Equations (2) and (3), K_r and K_θ are the constants of the harmonic oscillator. Also, r_0 and θ_0 are the equilibrium values of bond length and angle, respectively. Harmonic oscillator constants (K_r and K_θ) in the DREIDING force field are set to 700 (kcal/mol)/ Å^2 for each atomic bond and 100 (kcal/mol)/degree^2 for all bond angle bends. Furthermore, the equilibrium value of bond length and angle in our simulated structures is listed in **Table 2**[39].

Table 2. The r_0 and θ_0 values for the bond strength and angle bend of simulated structures by MD method[39].

Parameter	r_0 (Å)	θ_0 (degree)
C-O bond	1.420	-
O-O bond	1.310	-
O-C-O angle	-	109.471

As mentioned before, Tersoff force-field used for C atoms interaction in graphene nanosheets as below[38]:

$$E = \frac{1}{2}\sum_i \sum_{j \neq i} E_{ij} \tag{4}$$

$$E_{ij} = f_C(r_{ij})[f_R(r_{ij}) + b_{ij}f_A(r_{ij})] \tag{5}$$

where f_R is a two-body term and f_A includes three-body interactions. The summations in Equation (5) are over all neighbors j and k of atom i within a cutoff radius. After defining an appropriate force field for the O_2-CO_2 gas mixture and graphene-based membrane, MD study was fulfilled. Then, to describe the atomic structures time evolution inside the MD box, Newton's laws are used as the gradient of selected force-fields[35]:

$$F_i = \sum_{i \neq j} F_{ij} = m_i \frac{d^2 r_i}{dt^2} = m_i \frac{dv_i}{dt} \quad (6)$$

$$F_{ij} = -\nabla V_{ij} \quad (7)$$

From these base equations, the atomic momentum P_i can be defined as Equation (8)[37]:

$$P_i = m_i v_i \quad (8)$$

In the stated equations, to integrate the Newton's law's, the association of equation (6) is done by the Velocity-Verlet algorithm as below[35]:

$$r(t + \delta t) = r(t) + v(t)\delta t + \frac{1}{2} a(t)\delta t^2 \quad (9)$$

$$v(t + \delta t) = v(t) + \frac{1}{2}[a(t) + a(t + \delta t)]\delta t \quad (10)$$

In Equations (9) and (10), $r(t + \delta t)$, $v(t + \delta t)$ is the position and velocity of atoms in $t + \delta t$ and $r(t)$ and $v(t)$ are the values of these physical quantities in t. Furthermore, in the MD simulation approach, Gaussian distribution is implemented for temperature calculation in atomic arrangement as in Equation (11)[35]:

$$\frac{3}{2} k_B T = \frac{1}{N_{atom}} \sum_{i=1}^{N} \frac{1}{2} m v_i^2 \quad (11)$$

Finally, the instantaneous temperature variation is calculated from Equation (12)[35]:

$$T(t) = \sum_{i}^{N} \frac{m_i v_i^2(t)}{k_B N_{sf}} \quad (12)$$

where N_{sf} is the degree of freedom of the atomic systems. According to the reported descriptions, MD simulations in the current computational study were carried out as below:

- Step 1: CO_2-O_2 gas mixture and graphene-based membrane were simulated with DREIDING and Tersoff force fields and equilibrated by NVT ensemble for 1,000,000 time steps with Δt = 1 fs. For this purpose, atomic structures are set at a temperature of T_0 = 300 K as an initial condition. After atomic structures reached the equilibrium phase, the stability of them was reported by temperature and potential energy calculations.
- Step 2: Next, atomic purification process settings were implemented to equilibrate structures for 1,000,000 time steps with the NVE ensemble (t = 1 ns). For this purpose, a dynamic graphene sheet displaces in the MD simulation box with constant velocity (see **Figure 2**). After this process, physical parameters such as purification and permeability values are reported to describe the atomic behavior of graphene-based membranes in the O_2 purification process.

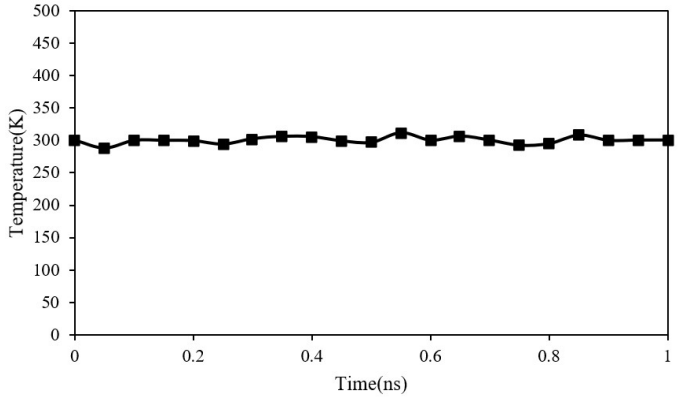

Figure 2. Temperature changes of graphene membrane and CO_2-O_2 gas mixture as a function of MD simulation time.

3. Results and discussion

3.1. Equilibration process of atomic structures

In the first step of our computational work, the atomic behavior of the O_2-CO_2 gas mixture and graphene-based membrane was studied at an initial temperature (T_0 = 300 K) for 1 ns. Our simulation results showed the initial arrangement of particles in the simulation box adopted with DREIDING and Tersoff force-fields[38,39]. This atomic phase of simulated structures is reported by temperature and potential energy calculations. The simulated structure's temperature changes as a function of simulation time as depicted in **Figure 2**. From calculated results, we conclude the atomic structures equilibrated after 1,000,000 time steps (t = 1 ns). Physically, this thermal equilibrium arises from atomic oscillation reducing, which indicated our MD simulation settings validity[35]. Also, **Figure 3** shows the potential energy changes in atomic systems as a function of MD simulation time in this computational step. From this figure, we conclude the simulated structure's potential energy converged after 1,000,000 time steps to a constant value. Numerically, the potential energy of the graphene membrane and CO_2-O_2 gas mixture reached −399 eV after 1 ns. Theoretically, this physical parameter has a reciprocal relation to the mean distance of atoms. By increasing the potential energy magnitude, the atomic stability of the target system increased. **Figure 3** indicated that by increasing the initial porous radius (R) from 3 Å to 5 Å and 7 Å, the atomic system isn't disrupted, and so, a stable phase of them can be detected after the equilibrium process. Our calculations show the temperature of equilibrated structures reaches 300 K in the final step of simulations. Physically, atomic stability of the initial membrane decreases with increasing porous radius. Numerically, by porous enlarging, the magnitude of the potential energy parameter decreases to −376.81 eV from −406.69 eV. This behavior arises from a carbon atom missing in the membrane structure, and interatomic force (by attraction type) decreases in the defined layer system. Atomic layer distance between graphene sheets (D) is another important parameter for graphene-based membrane stability. By this parameter, changes from 5 Å to 7.5 Å and 10 Å, the potential energy of the total atomic system decreases to −402.70 eV and −397.97 eV, respectively. This behavior arises from mutual interaction between carbon atoms, which causes saving energy in the MD simulation box. We can say the atomic stability of the simulated membrane decreased by these potential energy's magnitude decreasing.

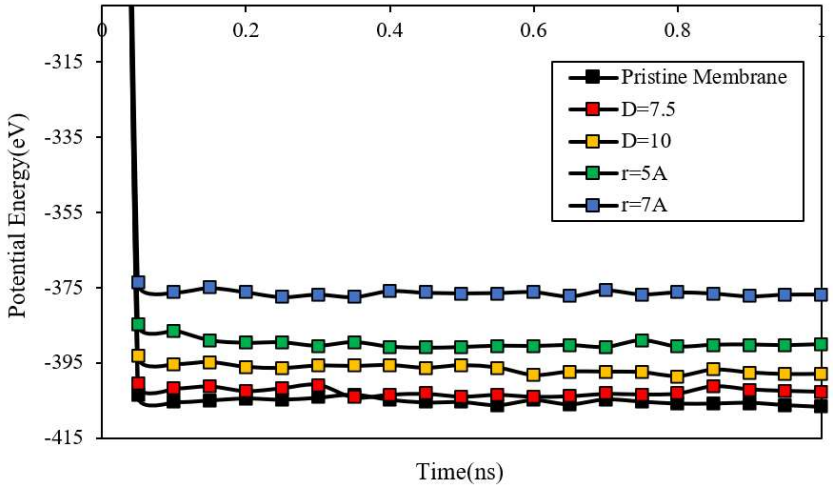

Figure 3. Potential energy changes of graphene membrane and CO_2-O_2 gas mixture as a function of porous radius and atomic layers distance.

3.2. Atomic behavior of simulated structures

3.2.1. Atomic behavior of pristine graphene membrane

In this step, MD settings were implemented to pristine graphene membranes to study the O_2 molecules purification efficiency with this atomic arrangement. **Figure 4** shows the evolution of atomic structures after 320,000 time steps (t = 0.32 ns). After the equilibration phase, the number of filtered O_2 molecules variation as a function of MD simulation time is reported in **Figure 5**. From this computational result, we conclude the MD simulation time (t = 1 ns) is long enough for the atomic purification process detecting. After this atomic phase, the number of CO_2 molecules that passed from the graphene membrane was reported (see **Figure 6**). From our MD simulation results, the number of filtered O_2 molecules reaches 603 (90.00% ratio), which this calculated value is comparable with previous reports[41,42]. Also computed, the value of CO_2 molecules that passed from the pristine membrane is 11 molecules (15.71% ratio). Reported atomic behavior of simulated structures in this MD simulation step shows the validity of our computational settings and shows the appropriate behavior of graphene-based membranes in the atomic purification process.

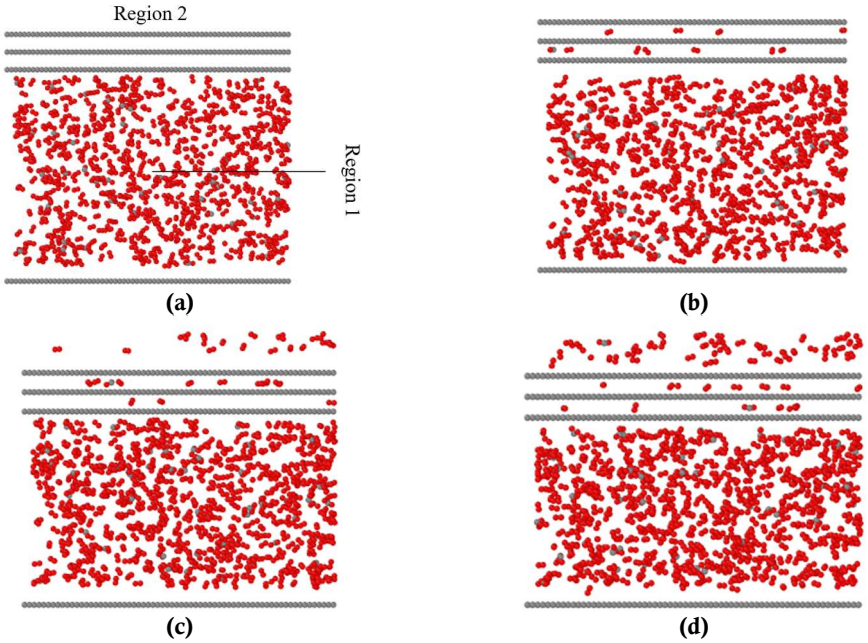

Figure 4. Time evolution of O_2-CO_2 gas mixture purification process with pristine graphene membrane. **(a)** t = 0; **(b)** t = 0.1 ns; **(c)** t=0.2 ns; **(d)** t = 0.3 ns.

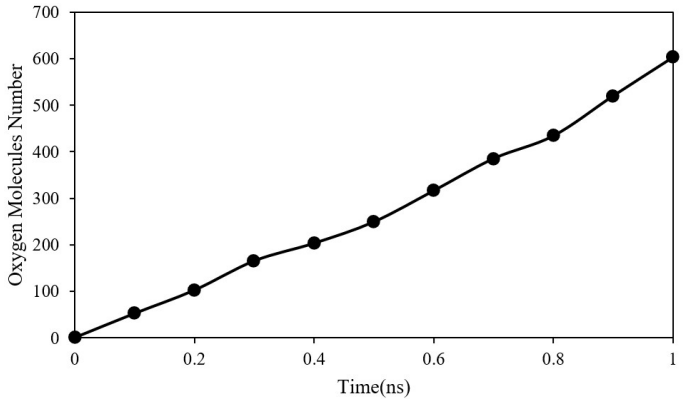

Figure 5. Number of O_2 molecules which passed from pristine graphene membrane as a function of MD simulation time.

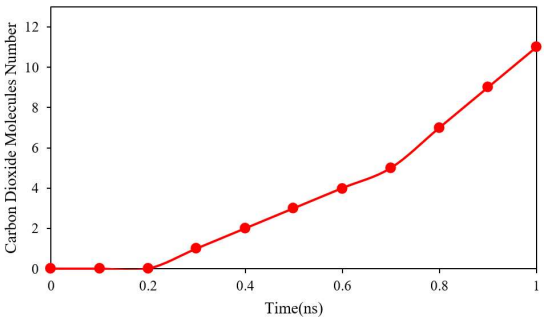

Figure 6. Number of CO_2 molecules which passed from pristine graphene membrane as a function of MD simulation time.

3.2.2. Graphene layers distance effect on atomic behavior of membrane

The results of graphene layer distance effects on carbon-based membrane purification behavior are reported in this section of our MD study. The distances of atomic layers (D) depicted in **Figure 1** are set to 5 Å, 7.5 Å, and 10 Å in the NVT ensemble by setting the initial temperature in T_0 = 300 K. After the atomic equilibration process simulation for 1,000,000 time steps (t = 1 ns), the atomic structure was used for the atomic purification process to estimate the efficiency of them in this performance. Numerically, by D parameter increasing, the number of O_2 molecules that passed from the carbon-based membrane decreases to 498 molecules (74.33% ratio) as reported in **Figure 7**. Furthermore, the CO_2 molecules elimination rate improves by D parameter increasing in the modeled atomic membrane, and the number of CO_2 molecules in region 2 reaches zero after 1 ns, as depicted in **Figure 8**. Physically, by graphene layer distance variation, the attraction force that is implemented to the O_2-CO_2 gas mixture changes. This type of atomic interaction decreases with increasing D parameter, and so the efficiency of the graphene membrane improved. Also, the permeability of atomic structures is affected by D parameter variation. From **Figure 9a** we can say the maximum value of this physical parameter reaches 62 L/cm^2/day/MPa and 43 L/cm^2/day/MPa by D parameter increasing from 7.5 Å to 10 Å, respectively. Here, the interaction energy between membrane atoms and gas mixtures is reported for more description of detected atomic phenomena. This physical parameter indicated the atomic evolution of simulated structures. We report the total component of interaction energy in **Figure 9b**. MD results show that by D parameter enlarging, the interaction energy between the membrane and O_2-CO_2 system decreases. This behavior arises from atomic distance increasing between simulated components, which, by this atomic evolution, the membrane efficiency decreases. As reported in **Figure 9b**, D parameter enlarging causes interaction energy changes from −41.32 eV to −32.09 eV. By analyzing data from this section of our MD simulations, we conclude that the D parameter increases, improves the accuracy of the atomic purification process, and decreases the speed of this atomic phenomenon (as listed in **Table 3**).

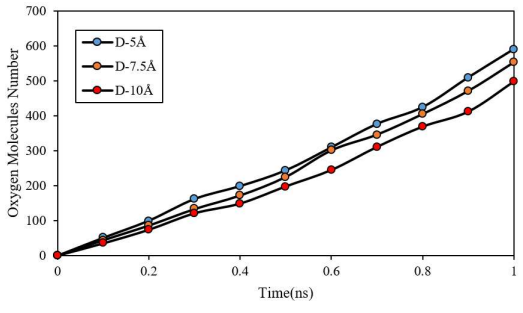

Figure 7. Number of O_2 molecules which passed from pristine graphene membrane as a function of graphene layers distance (D). The total number of O_2 molecules inside MD box is 670 molecules.

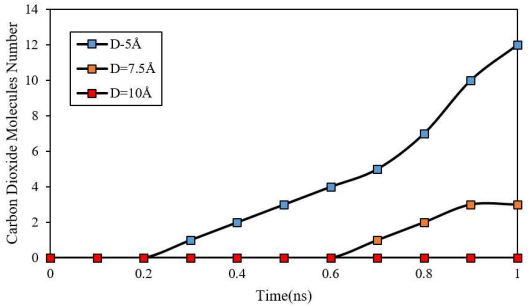

Figure 8. Number of CO2 molecules which passed from pristine graphene membrane as a function of graphene layers distance (D). The total number of CO_2 molecules inside MD box is 70 molecules.

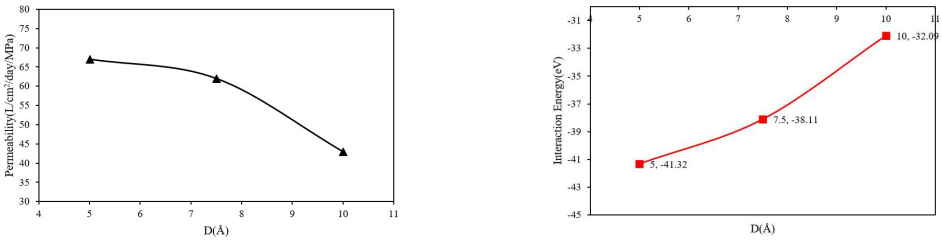

(a) **(b)**

Figure 9. (a) permeability of graphene-based membrane as a function of graphene layers distance (D); **(b)** interaction energy between atomic membrane and gas system as a function of D parameter.

Table 3. Number of O_2 and CO_2 molecules which passed from graphene-based membrane and membrane permeability as a function of graphene layers distance (D).

Graphene layers distance (Å)	Number of passed O_2 molecules	Number of passed CO_2 molecules	Permeability ($L/cm^2/day/MPa$)
5	591	12	67
7.5	553	3	62
10	498	0	43

3.2.3. Graphene layers porous size effect on atomic behavior of membrane

In the final step of our computational work, we reported the graphene layer's porous size (R) effect on carbon-based membrane purification efficiency. The porous size of graphene sheets is set to 3 Å, 5 Å, and 7 Å at T_0 = 300 K. After the MD equilibration process was implemented for t = 1 ns, the dynamic graphene sheet moved by 1 MPa pressure, and so the atomic purification process was fulfilled after 1 ns. Our MD simulation results show that, by R parameter increasing, the number of O_2 molecules in region 2 increases from 591 molecules (88.21%) to 623 (92.98%) and 652 (97.31%) molecules (respectively) as reported in **Figure 10**. Furthermore, the CO_2 molecules elimination rate is getting worse as the R parameter increases in graphene nanosheets. Numerically, CO_2 molecule elimination reaches 24.28% and 32.86% after 1 ns, as depicted in **Figure 11**. Physically, by graphene layers increasing in porous size, the atomic interaction between carbon atoms in membrane structure and O_2-CO_2 gas mixture decreased, and more molecules can be passed from graphene configuration as a target membrane. The permeability of the graphene membrane is also affected by R parameter variation, and the maximum value of this atomic separation factor reaches 71 $L/cm^2/day/MPa$ and 77 $L/cm^2/day/MPa$ (see **Figure 12a**). As in the previous section, the interaction energy between the atomic membrane and the atomic gas mixture is reported in **Figure 12b**. MD outputs in this section indicated the interaction energy gets to more values by R parameter enlarging. By this process occurring, the number of atoms that were attracted by graphene sheets increased, and the number of

passed molecules from the target membrane improved. From these calculated results, we can conclude that increasing the R parameter decreases the accuracy of the purification process and increases the speed of this atomic phenomenon, as reported in **Table 4**.

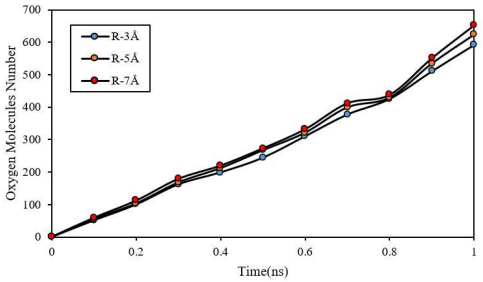

Figure 10. Number of O_2 molecules which passed from pristine graphene membrane as a function of graphene layers porous size (R).

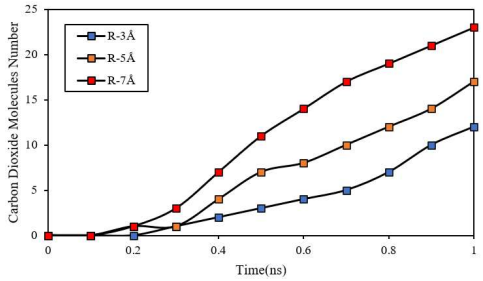

Figure 11. Number of CO_2 molecules which passed from pristine graphene membrane as a function of graphene layers porous size (R).

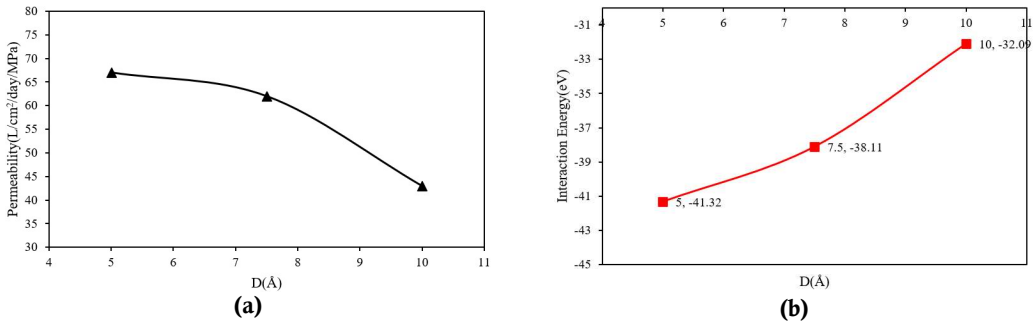

Figure 12. (a) Permeability of graphene-based membrane as a function of graphene layers porous size (R); **(b)** interaction energy between atomic membrane and gas system as a function of R parameter.

Table 4. Number of O_2 and CO_2 molecules which passed from graphene-based membrane and membrane permeability as a function of graphene layers porous size (R).

Graphene layers porous size (Å)	Number of passed O_2 molecules	Number of passed CO_2 molecules	Permeability (L/cm²/day/MPa)
3	591	12	67
5	623	17	71
7	652	23	77

4. Conclusion

We use Molecular Dynamics (MD) simulations to describe the behavior of multilayer (3-layer) graphene membranes in the gas mixture purification process (O_2 molecules purification from the O_2-CO_2 gas system). Our important computational results from MD simulations are as follows:

- DREIDING and Tersoff force fields are appropriate functions for MD simulation of graphene-based membranes and O_2-CO_2 gas mixtures inside MD boxes.
- MD outputs predicted the number of O_2 and CO_2 molecules that passed from the graphene membrane are 652 (97.31% ratio) and 23 (32.86% ratio) molecules after t = 1 ns.
- Numerically, the permeability of the graphene membrane reaches a 77 L/cm^2/day/MPa value by atomic structure optimization.
- Increasing the distance of graphene atomic layers in the simulated membrane causes the accuracy to improve and performance speed to decrease in the atomic purification process. Numerically, the interaction energy between the membrane and gas mixture converged to −09 eV by this atomic process done.
- Increasing the number of graphene atomic layers is porous, causing the accuracy to decrease and performance speed to increase in the atomic purification process. Numerically, the interaction energy between the membrane and gas mixture converged to −93 eV by this atomic process done.

These MD simulation results show that the atomic arrangement of carbon atoms in graphene-based membranes can improve the purification process accuracy or speed. Practically, these estimated results can be implemented in various purification processes to optimize industrial application efficiency.

Author contributions

Conceptualization, MPP and BPA; methodology, MPP and BPA; software, MPP and BPA; validation, MPP and BPA; formal analysis, MPP and BPA; investigation, MPP and BPA; resources, MPP and BPA; data curation, MPP and BPA; writing—original draft preparation, MPP and BPA; writing—review and editing, RS; visualization, MPP and BPA; supervision, RS; project administration, RS; funding acquisition, RS. All authors have read and agreed to the published version of the manuscript.

Conflict of interest

The authors declare no conflict of interest.

Nomenclature

F_{ij}	Atomic force between i and j atoms;
V_{ij}	Potential energy between i and j atoms;
m	Atomic mass;
r_c	Cut-off radius;
r_{ij}	Distance between i and j atoms;
t	Time step in molecular dynamics simulation;
T	Temperature in molecular dynamics simulation;
v	Atomic velocity;
N_{atom}	Number of atoms;
N_{sf}	Degree of freedom;
k_B	Boltzman constant;
r_0	Equilibrium bond length;
ε	Energy constant in Lennard-Jones function;
σ	Length constant in Lennard-Jones function;
θ_0	Equilibrium angle.

References

1. Bunch JS, Verbridge SS, Alden JS, et al. Impermeable Atomic Membranes from Graphene Sheets. Nano Letters. 2008; 8(8): 2458-2462. doi: 10.1021/nl801457b
2. Gilje S, Han S, Wang M, et al. A Chemical Route to Graphene for Device Applications. Nano Letters. 2007; 7(11): 3394-3398. doi: 10.1021/nl0717715
3. Schniepp HC, Li JL, McAllister MJ, et al. Functionalized Single Graphene Sheets Derived from Splitting Graphite Oxide. The Journal of Physical Chemistry B. 2006; 110(17): 8535-8539. doi: 10.1021/jp060936f
4. Zhou F, Fathizadeh M, Yu M. Single- to Few-Layered, Graphene-Based Separation Membranes. Annual Review of Chemical and Biomolecular Engineering. 2018; 9(1): 17-39. doi: 10.1146/annurev-chembioeng-060817-084046
5. Geim AK, Novoselov KS. The rise of graphene. Nature Materials. 2007; 6(3): 183-191. doi: 10.1038/nmat1849
6. Peres NMR, Ribeiro RM. Focus on graphene. New Journal of Physics. 2009; 11(9): 095002. doi: 10.1088/1367-2630/11/9/095002
7. Boehm HP, Setton R, Stumpp E. Nomenclature and terminology of graphite intercalation compounds (IUPAC Recommendations 1994). Pure and Applied Chemistry. 1994; 66(9): 1893-1901. doi: 10.1351/pac199466091893
8. Harris P. Transmission Electron Microscopy of Carbon: A Brief History. C. 2018; 4(1): 4. doi: 10.3390/c4010004
9. Nair RR, Blake P, Grigorenko AN, et al. Fine Structure Constant Defines Visual Transparency of Graphene. Science. 2008; 320(5881): 1308-1308. doi: 10.1126/science.1156965
10. Lee C, Wei X, Kysar JW, et al. Measurement of the Elastic Properties and Intrinsic Strength of Monolayer Graphene. Science. 2008; 321(5887): 385-388. doi: 10.1126/science.1157996
11. Tsang ACH, Kwok HYH, Leung DYC. The use of graphene based materials for fuel cell, photovoltaics, and supercapacitor electrode materials. Solid State Sciences. 2017; 67: A1-A14. doi: 10.1016/j.solidstatesciences.2017.03.015
12. Qu L, Liu Y, Baek JB, et al. Nitrogen-Doped Graphene as Efficient Metal-Free Electrocatalyst for Oxygen Reduction in Fuel Cells. ACS Nano. 2010; 4(3): 1321-1326. doi: 10.1021/nn901850u
13. Vivekchand SRC, Rout CS, Subrahmanyam KS, et al. Graphene-based electrochemical supercapacitors. Journal of Chemical Sciences. 2008; 120(1): 9-13. doi: 10.1007/s12039-008-0002-7
14. Zhang LL, Zhou R, Zhao XS. Graphene-based materials as supercapacitor electrodes. Journal of Materials Chemistry. 2010; 20(29): 5983. doi: 10.1039/c000417k
15. Li H, Zou L, Pan L, et al. Novel Graphene-Like Electrodes for Capacitive Deionization. Environmental Science & Technology. 2010; 44(22): 8692-8697. doi: 10.1021/es101888j
16. Zhang D, Yan T, Shi L, et al. Enhanced capacitive deionization performance of graphene/carbon nanotube composites. Journal of Materials Chemistry. 2012; 22(29): 14696. doi: 10.1039/c2jm31393f
17. Yin H, Zhao S, Wan J, et al. Three-Dimensional Graphene/Metal Oxide Nanoparticle Hybrids for High‐Performance Capacitive Deionization of Saline Water. Advanced Materials. 2013; 25(43): 6270-6276. doi: 10.1002/adma.201302223
18. Cohen-Tanugi D, Grossman JC. Water Desalination across Nanoporous Graphene. Nano Letters. 2012; 12(7): 3602-3608. doi: 10.1021/nl3012853
19. You Y, Sahajwalla V, Yoshimura M, et al. Graphene and graphene oxide for desalination. Nanoscale. 2016; 8(1): 117-119. doi: 10.1039/c5nr06154g
20. Cohen-Tanugi D, Lin LC, Grossman JC. Multilayer Nanoporous Graphene Membranes for Water Desalination. Nano Letters. 2016; 16(2): 1027-1033. doi: 10.1021/acs.nanolett.5b04089
21. Xue C, Wang X, Zhu W, et al. Electrochemical serotonin sensing interface based on double-layered membrane of reduced graphene oxide/polyaniline nanocomposites and molecularly imprinted polymers embedded with gold nanoparticles. Sensors and Actuators B: Chemical. 2014; 196: 57-63. doi: 10.1016/j.snb.2014.01.100
22. Asgari A, Nguyen Q, Karimipour A, et al. Investigation of additives nanoparticles and sphere barriers effects on the fluid flow inside a nanochannel impressed by an extrinsic electric field: A molecular dynamics simulation. Journal of Molecular Liquids. 2020; 318: 114023. doi: 10.1016/j.molliq.2020.114023
23. Ashkezari AZ, Jolfaei NA, Jolfaei NA, et al. Calculation of the thermal conductivity of human serum albumin (HSA) with equilibrium/non-equilibrium molecular dynamics approaches. Computer Methods and Programs in Biomedicine. 2020; 188: 105256. doi: 10.1016/j.cmpb.2019.105256
24. Ghanbari A, Warchomicka F, Sommitsch C, et al. Investigation of the Oxidation Mechanism of Dopamine Functionalization in an AZ31 Magnesium Alloy for Biomedical Applications. Coatings. 2019; 9(9): 584. doi: 10.3390/coatings9090584

25. Sabetvand R, Ghazi ME, Izadifard M. Studying temperature effects on electronic and optical properties of cubic CH3NH3SnI3 perovskite. Journal of Computational Electronics. 2020; 19(1): 70-79. doi: 10.1007/s10825-020-01443-3
26. Cohen-Tanugi D, Grossman JC. Water Desalination across Nanoporous Graphene. Nano Letters. 2012; 12(7): 3602-3608. doi: 10.1021/nl3012853
27. Cohen-Tanugi D, Lin LC, Grossman JC. Multilayer Nanoporous Graphene Membranes for Water Desalination. Nano Letters. 2016; 16(2): 1027-1033. doi: 10.1021/acs.nanolett.5b04089
28. Kim HW, Yoon HW, Yoon SM, et al. Selective Gas Transport Through Few-Layered Graphene and Graphene Oxide Membranes. Science. 2013; 342(6154): 91-95. doi: 10.1126/science.1236098
29. Wang J, Zhang P, Liang B, et al. Graphene Oxide as an Effective Barrier on a Porous Nanofibrous Membrane for Water Treatment. ACS Applied Materials & Interfaces. 2016; 8(9): 6211-6218. doi: 10.1021/acsami.5b12723
30. Plimpton S. Fast Parallel Algorithms for Short-Range Molecular Dynamics. Journal of Computational Physics. 1995; 117(1): 1-19. doi: 10.1006/jcph.1995.1039
31. Plimpton SJ, Thompson AP. Computational aspects of many-body potentials. MRS Bulletin. 2012; 37(5): 513-521. doi: 10.1557/mrs.2012.96
32. Aktulga HM, Fogarty JC, Pandit SA, et al. Parallel reactive molecular dynamics: Numerical methods and algorithmic techniques. Parallel Computing. 2012; 38(4-5): 245-259. doi: 10.1016/j.parco.2011.08.005
33. Brown WM, Wang P, Plimpton SJ, et al. Implementing molecular dynamics on hybrid high performance computers – short range forces. Computer Physics Communications. 2011; 182(4): 898-911. doi: 10.1016/j.cpc.2010.12.021
34. Stukowski A. Visualization and analysis of atomistic simulation data with OVITO–the Open Visualization Tool. Modelling and Simulation in Materials Science and Engineering. 2009; 18(1): 015012. doi: 10.1088/0965-0393/18/1/015012
35. Rapaport DC. The Art of Molecular Dynamics Simulation, 2nd ed. Cambridge University Press; 2004.
36. Nosé S. A unified formulation of the constant temperature molecular dynamics methods. The Journal of Chemical Physics. 1984; 81(1): 511-519. doi: 10.1063/1.447334
37. Hoover WG. Canonical dynamics: Equilibrium phase-space distributions. Physical Review A. 1985; 31(3): 1695-1697. doi: 10.1103/physreva.31.1695
38. Mayo SL, Olafson BD, Goddard WA. DREIDING: a generic force field for molecular simulations. The Journal of Physical Chemistry. 1990; 94(26): 8897-8909. doi: 10.1021/j100389a010
39. Tersoff J. New empirical approach for the structure and energy of covalent systems. Physical Review B. 1988; 37(12): 6991-7000. doi: 10.1103/physrevb.37.6991
40. Lennard-Jones JE. On the Determination of Molecular Fields. Proceedings of the Royal Society of London. 1924; 106(738): 463-477.
41. Cohen-Tanugi D, Grossman JC. Water permeability of nanoporous graphene at realistic pressures for reverse osmosis desalination. The Journal of Chemical Physics. 2014; 141(7). doi: 10.1063/1.4892638
42. Nair RR, Wu HA, Jayaram PN, et al. Unimpeded Permeation of Water Through Helium-Leak–Tight Graphene-Based Membranes. Science. 2012; 335(6067): 442-444. doi: 10.1126/science.1211694